OUTPUT BASED INPUT SHAPING FOR OPTIMAL CONTROL OF SINGLE LINK FLEXIBLE MANIPULATOR

Nura Musa Tahir[1,2], Sabo Miya Hassan[1*], Zaharuddin Mohamed[2] and Ahmed Garba Ibrahim[1].

[1]Faculty of Engineering, Abubakar Tafawa Balewa University, PMB 0248, Bauchi, Nigeria

[2]Faculty of Electrical Engineering, Universiti Teknologi Malaysia, 81310 UTM, Johor, Malaysia

Emails: *hsmiya2010@gmail.com, nuratahir85@gmail.com

Submitted: Mar 10, 2017 ***Accepted: Apr. 17, 2017*** ***Published: June 1, 2017***

Abstract- Endpoint residual vibrations and oscillations due to flexible and rigid body motions are big challenges in control of single link flexible manipulators, it makes positioning of payload difficult especially when using various payloads. This paper present output based input shaping with two different control algorithms for optimal control of single link flexible manipulators. Output based filter (OBF) is designed using the signal output of the system and then incorporated with both linear quadratic regulator (LQR) and PID separately for position and residual vibration control. The Robustness of these control algorithms are tested by changing the payloads from 0g to30g, 50g and 70g in each case. Based on MATLAB simulation results and time response analysis, LQR-OBF outperformed the PID-OBF in both tracking and vibration reduction.

Index terms*:* Single link flexible manipulator, residual vibrations, input shaping, linear quadratic regulator (LQR), PID controller, optimal control.

I. INTRODUCTION

Flexible manipulators are equipment designed to move objects from one point to another. Light weight flexible manipulators consume less power, and are cheaper and faster than their heavy rigid counterparts. Hence, they are used for various applications such as spray painting, welding, automatic micro-assembling, semiconductor manufacturing and so on. Flexible manipulators are thus used in many industries such as automotive, nuclear power plant, aerospace and space exploration[1, 2]. However, because of their flexible nature, these manipulators are prone to residual vibrations and oscillations due to flexible and rigid body motions of the system. This makes payload positioning difficult, especially when moving payloads of varying weight. Thus, due to these problems, various control approaches have been proposed by many researchers using control schemes such as feedback, feedforward, hybrid and robust controllers.

In feedforward control, various input shaping methods for the control of tip deflections and vibrations were presented in[3], and their performance were assessed based on level of vibration reduction, response time analysis and robustness. In [4], microcontroller based input shaping for the control of residual vibration is presented, assumed mode method is used to drive the dynamic model of the system and embedded input shaping performances and applications are compared. In [5], command shaping control techniques for vibration suppression was presented. Input shaping, low pass and band stop filters are experimentally investigated and assessed. Input shaping for eliminating vibrations using an offline learning method was proposed in [6]. The method proved effective and no additional sensor is required. Output-based input shaping for vibration control was presented in [7]. It is designed using the signal output of the target system, thus in addition to being robust, the problems of parameter uncertainty are avoided. In addition, various types of input shaping techniques, zero vibration (ZV), zero vibration derivative (ZVD) and zero vibration derivative-derivative (ZVDD) to suppress residual vibrations and oscillations have been proposed in [2, 7-10]. PID control is very popular in the industry for feedback control [11]. Foe feedback rigid body motion control of a single link flexible manipulator using PID was presented in [12].

In hybrid control, experimental investigations of hybrid input shaping and PID control of tip deflection and input tacking was presented in [13]. The performance of ZV-PID and ZVDD-PID was assessed based on input tracking and vibration reduction. In [14], pneumatic drive active

vibration control using an adaptive interactive PD controller was proposed. Pneumatic drive system is used as actuator which was used to control rigid body motion while adaptive interactive PD is also used for vibration and position control. Simulation and experimental results proved the effectiveness of this technique. A composite fuzzy logic control strategy using PD, PID and ZVDD for input tracking and vibration suppression are proposed in [15]. The control scheme's performance was assessed based on input tracking, vibration reduction and time response analysis. The use of optimal control such as LQR and LQG have been reported for robotic and other application [16, 17]. The flexible maneuvering system which also falls within the robotics application is prone to vibration at its end point. Thus, different techniques for vibration reduction and input tracking was proposed in [18], LQR, LQR-PID and LQR–Input shaping was designed to control the hub angle and suppress residual vibrations in the system. Vibration and input tracking control using LQR and non-collocated PID was proposed in [19]. In [20], a modified genetic algorithm using a tuned PD controller for vibration and input tracking control was proposed. Faster convergence and higher accuracy was achieved and the problem of premature convergence and stagnation were solved using this approach. In [21], feedback linearization and input shaping control strategy to eliminate residual vibrations was proposed. Simulation results proved the effectiveness of this technique.

In robust control, a control strategy robust to payload changes is presented in [22]. The control system was made up of two loops, the inner feedback loop to control the hub position while the outer loop (consisting of feed forward and feedback) to for control the tip deflection. Shape optimization of the revolute joint of the single link flexible manipulator for vibration suppression was presented in [23]. Various optimization problems were solved to study the performance of the model for vibration suppression.

This paper proposes a hybrid control scheme where an output-based filter is incorporated with LQR and PID separately for vibration and position control of a single link flexible manipulator. To test the robustness of the control schemes, the payload is varied from 0g to 30g, 50g and 70g and their performances are compared in each case. The rest of the paper is organized as follows; section II presents system description and modeling of a single link flexible manipulator, section III presents control algorithms, section IV discusses results and performance of control algorithms, and section V gives the conclusion.

II. SYSTEM DESCRIPTION AND MODEL OF SINGLE LINK FLEXIBLE MANIPULATOR

a. System Description

In this work, the flexible manipulator considered is the laboratory scale single –link flexible manipulator developed at the University of Sheffield shown in Fig 1. The model of the single link flexible manipulator was derived using finite element method as presented in [3, 5, 9, 24]. The simplified outline of the system is described in Figs. 2 and 3 respectively. There are movable and non-movable coordinates, XOY and X'OY' respectively. The values and definition of various parameters are as recorded in Table 1. Other parameters not defined in the table are the payload mass $M_{p,}$ hub angular displacement moving in XOY plane $\theta(t)$ and the hub driving motor torque $\tau(t)$. It should be noted that the single link flexible manipulator only moves in the XOY plane.

Figure 1. Flexible manipulator system experimental rig

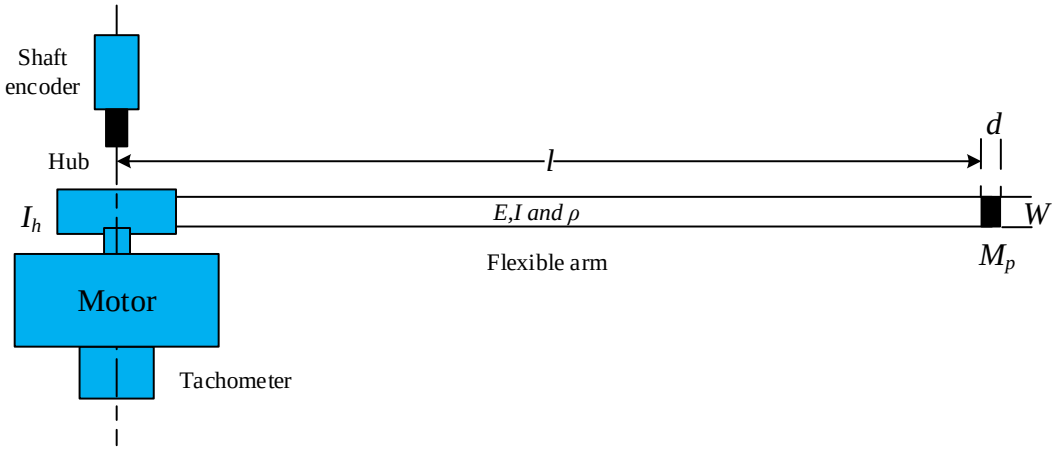

Figure 2. A simplified outline of the single-link flexible manipulator

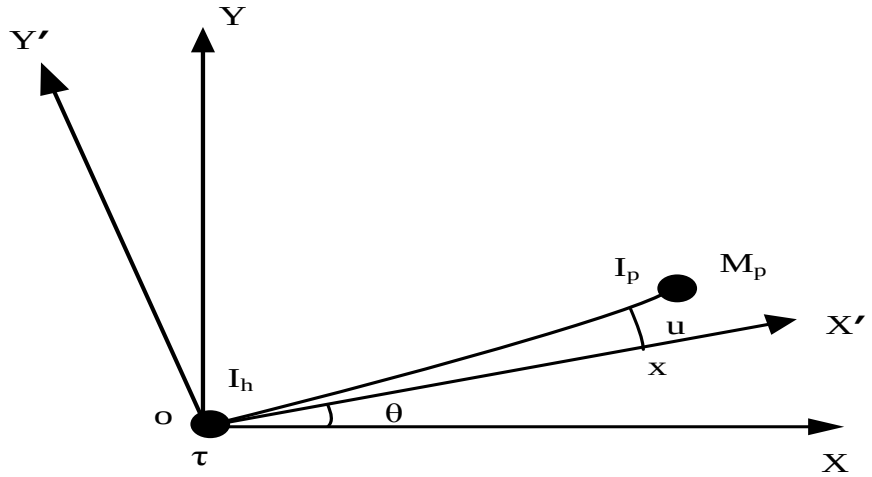

Figure 3. Schematic of the flexible manipulator system

Table 1 System Parameters

Parameters	**Symbols**	**Values**	**Units**
Young modulus	E	$71x10^{9}$	N/m^{2}
Mass density per unit volume	ρ	2710	Kg/m^{3}
Second moment of inertia	I	5.1924	m^{4}
Flexible link length	L	0.96	m
Flexible link width	W	0.019	m
Flexible link thickness	B	0.003	m
Hub inertia	I_h	5.86×10^{-4}	Kgm^2
Moment of inertia	I_b	5.1924	Kgm^2

b. Model of Single Link Flexible Manipulator

As mentioned in section II.a, finite element method was used with 10 numbers of elements to determine the dynamic behavior of the system. Hub inertia, payload and structural damping was also considered [6]. Since it is slender and long, rotary inertia effect and transverse shear are neglected. Elastic behavior of the system was modeled based on these assumptions using Bernoulli-Euler beam theory [3, 25]. Thus for an angular displacement θ(t) and a slight elastic deflection $u(x,t)$, the total displacement can be given as

$$y(x,t) = x\theta(t) + u(x,t) \tag{1}$$

Thus, the fourth order partial differential equation representing this motion can be written as

$$EI\frac{\partial^4 y(x,t)}{\partial x^4} + \rho\frac{\partial^2 y(x,t)}{\partial t^2} - D_s\frac{\partial^3 y(x,t)}{\partial x^2 \partial t} = 0 \tag{2}$$

where *Ds* is the damping constants and the matching boundary conditions are

$$\begin{aligned} &y(0,t) = 0 \\ &I_h\frac{\partial^3 y(0,t)}{\partial x^2 \partial x} - EI\frac{\partial^2 y(0,t)}{\partial x^2} = \tau(t) \\ &M_P\frac{\partial^2 y(l,t)}{\partial x^2} - EI\frac{\partial^3 y(l,t)}{\partial x^3} = 0 \\ &EI\frac{\partial^2 y(l,t)}{\partial x^2} = 0 \end{aligned} \tag{3}$$

while the initial condition are

$$\begin{aligned} &y(0,t) = 0 \\ &\frac{\partial y(x,0)}{\partial x} = 0 \end{aligned} \tag{4}$$

Solution to (2) is obtained using the finite element method leads to

$$u(x,t) = \mathbf{N}_r(x)\mathbf{Q}_r(t) \tag{5}$$

Where $\mathbf{N}_r(x)$ and $\mathbf{Q}_r(t)$ are the respective shape function and nodal displacement. Thus we can obtain the displacement as

$$y(x,t) = \mathbf{N}(x)\mathbf{Q}_s(t) \tag{6}$$

where $\mathbf{N}(x) = \begin{bmatrix} x & \mathbf{N}_s(t) \end{bmatrix}$ and $\mathbf{Q}_s(t) = \begin{bmatrix} \theta(t) & \mathbf{Q}_r(t) \end{bmatrix}^T$

Accordingly, using the kinetic and potential energies of an element, and defining a local variable of the nth element as $k = x - \sum_{i=1}^{n-1} l_i$ where l_i is the ith element length. The element mass matrix $\mathbf{M}_n$ and stiffness matrix $\mathbf{K}_n$ are obtained as

$$\mathbf{M}_n = \int_0^l \rho A(\mathbf{N}^T\mathbf{N})dk \tag{7}$$

$$\mathbf{K}_n = \int_0^l EI(\mathbf{\Phi}^T\mathbf{\Phi})dk \tag{8}$$

where $\mathbf{\Phi} = \dfrac{d^2\mathbf{N}(k)}{dk^2}$.

The respective elements mass and stiffness matrices $\mathbf{M}_n$ and $\mathbf{K}_n$ are assembled to form the systems mass and stiffness matrices **M** and **K** respectively. These new matrices are used in the Lagrange equation to obtain the dynamic equation of the manipulator as follows

$$\mathbf{M}\ddot{\mathbf{Q}}(t) + \mathbf{D}\dot{\mathbf{Q}}(t) + \mathbf{K}\mathbf{Q}(t) = \mathbf{F}(t) \tag{9}$$

where **D** is the damping matrix, $\mathbf{F}(t)$ is the external forces vector and $\mathbf{Q}(t)$ is the nodal displacement vector from (6) given as $\mathbf{Q}(t) = \begin{bmatrix} \theta & u_0 & \theta_0 & \ldots & u_n & \theta_n \end{bmatrix}^T$ where, $u_n(t)$ and $\theta_n(t)$ are the end point flexural and angular deflections respectively. **M** and **K** matrices are of dimension *m* x *m and* F *is* of dimension *m* x *1*.

Equation (9) can be written in state space as ;

$$\dot{x} = \mathbf{A}x + \mathbf{B}u$$
$$y = \mathbf{C}x \qquad (10)$$

where,

$$\mathbf{A} = \begin{bmatrix} 0_m & I_m \\ -M^{-1}K & -M^{-1}D \end{bmatrix}, \quad \mathbf{B} = \begin{bmatrix} 0_{m\times 1} \\ M^{-1} \end{bmatrix}, \text{ and } \mathbf{C} = \begin{bmatrix} I_m & 0_m \end{bmatrix}.$$

where, I_m is an identity matrix and 0_m a null matrix both of the same dimension as M and K. 0_{mx1} is a null vector of dimension $mx1$.Thus, for position and residual vibration control, $m= 2$ and after substituting the respective value of the parameters given in Table 1, the A, B and C matrices are obtained as follows

$$A = \begin{bmatrix} 0 & 0 & 1 & 0 \\ 0 & 0 & 0 & 1 \\ 0 & 58209 & 0 & -33 \\ 0 & -38548 & 0 & -27 \end{bmatrix}, \quad B = \begin{bmatrix} 0 \\ 0 \\ 1013.6 \\ -821 \end{bmatrix}, \quad C = \begin{bmatrix} 1 & 0 & 0 & 0 \\ 0 & 1 & 0 & 0 \end{bmatrix},$$

III. CONTROLLER DESIGN

In this section, the output-based input shaping filter, LQR and PID are designed for both position and residual vibration control. The filter is incorporated with both controllers independently and in each case their performances are assessed. The block diagram of the PID control structure with the filter is shown in Fig. 4. In Fig. 5, a typical LQR control structure is shown as given in [16]. Adaptation of this structure to include the output based input shaping filter (OBF) is also shown in Fig. 6. Subsequently, the design for the OBF filter and the LQR are given in sections IIIa and IIIb respectively.

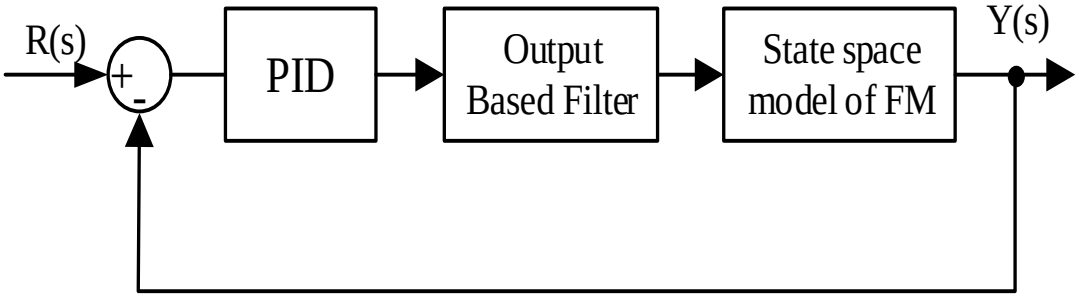

Figure 4. PID-OBF filter control structure of the Flexible manipulator

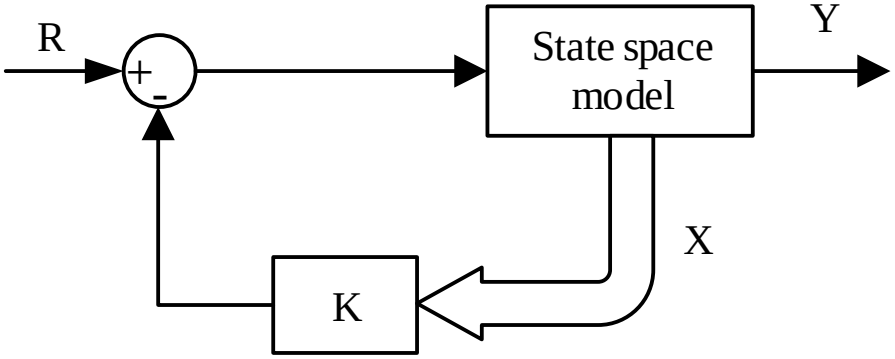

Figure 5. Typical LQR control system

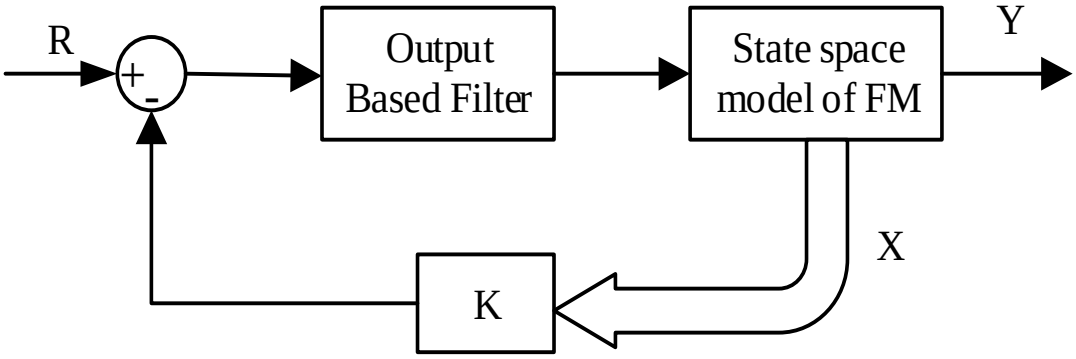

Figure 6. Flexible manipulator LQR-OBF control system

a. Output based Input Shaping

Unlike conventional input shaping in which natural frequency and damping ratio are used to calculate the filter's parameters, the output-based filter is designed using only signal output of the

target system. Hence the problem of parameter uncertainty is avoided. In this paper, a reference system used for the filter was designed based on the dynamic response of the single link flexible manipulator. To explain the basic principle of this technique, a second order system is considered as in [26].

$$G(s) = \frac{K\omega_n^2}{s^2 + 2\xi\omega_n^2 + \omega_n^2} \qquad (11)$$

Hence, the reference system is designed in the following form:

$$M(s) = \frac{k_m\omega_n^2}{s^2 + 2\xi_m\omega_m^2 + \omega_m^2} \qquad (12)$$

If an output shaping filter $F_0(s)$ is designed as:

$$F_0(s) = \frac{k_m\omega_n^2 s^2 + 2\xi\omega_n^2 + \omega_n^2}{K\omega_n^2 s^2 + 2\xi_m\omega_m^2 + \omega_m^2}, \qquad (13)$$

Such that the product of $G(s)$ and $F_0(s)$ will yield $M(s)$, thus

$$M(s) = F_0(s)G(s) \qquad (14)$$

Thus with zero-pole cancellation, the resulting system will be just like the reference system. Therefore, adequate static gain, damping ratio and bandwidth can be achieved by choosing k_m, ξ_m, ω_m respectively [26, 27].

Thus,

$$F(s) = \frac{s^2 a_2 + a_1 s + a_0}{s^2 + 2\xi_m w_m s + w_m^2} \qquad (15)$$

The aim The aim is to obtain the values of filter gains (a_o, a_1, a_2) so that zeros of $F(s)$ cancel the poles of $G(s)$ therefore, $F(s) = F_0(s)$ and poles of $G(s)$ are identical [26].

The reference system can be realized as:

$$G_r(s) = \frac{\omega_c^2}{(s + \omega_c)^2} \qquad (16)$$

where ω_c is the bandwidth of the system and is selected based on the time response of the system, this system has little or zero vibration. A cost function is used to minimize the difference between the output of the reference system and that of the target system [27].

$$E(s) = \omega(t)\int_0^T (\mathrm{y}(\mathrm{t}) - y_r(t))d_t \tag{17}$$

where, $\omega(t), y(t)$ and $y_r(t)$ are the weighting factor, output of the target system and output of the reference. Hence, decomposing output of the target system, equation (17) can be further elaborated as:

$$E(a_1 a_2, \ldots a_n) = \int_0^T \omega(t)\,((\sum_{i=0}^{m} a_i y_i(t)) - y_r(t))^2 \tag{18}$$

Thus, $a_1, a_2 \ldots a_m$ can be obtained from equation (9) and it is further simplified as:

$$\int_0^T \omega(t)\, y_k(t)\,((\sum_{i=0}^{m} a_i y_i(t)) - y_r(t))dt = 0 \tag{19}$$

Therefore, equation (10) can be realized as:

$$S_{\alpha,\beta} = \int_0^T \omega(t)\, y_\alpha(t)\, y_\beta(t), \quad \alpha = 0,1,2,3\ldots m \quad \beta = 0,1,2,3,\ldots m \quad \alpha + \beta \neq 0 \tag{20}$$

$$S_{\alpha,r} = \int_0^T w(t)\, y_\alpha(t)\, y_r(t), \quad \alpha = 0,1,2,3\ldots m \tag{21}$$

Hence, simplifying equations (10), (11) and (12) will give:

$$\sum_{i=0}^{m} a_k S_{k,i} - S_{k,r} = 0, \quad K = 0,1,2,3\ldots m \tag{22}$$

In this work, the single link flexible manipulator is type-2 system, hence, a_0 and a_1 are zero. The reference system was designed by considering the dynamic response of the system. Thus, selecting $\omega_c = 6$, using equation (16), the reference system is as:

$$G_r(s) = \frac{6^4}{(s+6)^4} \tag{23}$$

If (14) is further simplified,

$$G_r(s) = \frac{1296}{s^4 + 24s^3 + 216s^2 + 864s + 1296} \tag{24}$$

The filter gains a_2, a_3, a_4 are obtained by solving (25) below through a MATLAB program.

$$\begin{bmatrix} a_2 \\ a_3 \\ a_4 \end{bmatrix} = \begin{bmatrix} S_{22} & S_{23} & S_{24} \\ S_{32} & S_{33} & S_{34} \\ S_{42} & S_{43} & S_{44} \end{bmatrix} \begin{bmatrix} S_{2r} \\ S_{3r} \\ S_{4r} \end{bmatrix} \tag{25}$$

Thus, $a_0 = 0.5752, a_1 = -5.9820X10^9, a_2 = -8.1008X10^{-5}$

Substituting for a_2, a_3, a_4 in the filter equation we have

$$F(s) = \frac{-8.1008X10^{-5}s^4 - 5.9820X10^9 s^3 + 0.5752s^2}{s^4 + 24s^3 + 216s^2 + 864s + 1296} \tag{26}$$

b. LQR control

The LQR is an optimal controller that is very good in state and output regulations and input tracking [16]. It is a full state feedback controller. R is a weighting positive definite matrix which determines the control action of the system while Q is a positive semi-definite and directly affects the states of the system. These parameters are tuned to obtain the gain matrices K using the LQR MATLAB command. The performance index will be reduced so as to obtained optimal control [28].

Therefore,

$$J = \int_0^\infty (x^T(t)Q(t)x(t) + u^T(t)Ru(t) \tag{27}$$

Then, optimal *u* can be obtained using any initial state $x(0)$ as;

$$u = -Kx = -R^{-1}B^T Px(t) \tag{28}$$

Where, *P* is the solution of Riccati equation;

$$A^T P + PA - PBR^{-1}B^T P + Q = 0 \tag{29}$$

Using equation (28), the gain matrices can be obtained. However, as shown in Figs. 5 and 6 states sensors requirement is the main disadvantage of this control technique. $X(t)$ is the state variable multiplied by gain *K* and *u* is the desired input to the system. Fig. 6 shows a complete block diagram of the system.

IV. RESULTS AND DISCUSSIONS

The Single link flexible manipulator model is simulated to a bang-bang input torque of $\pm 90°$ reference angle to evaluate the performance of both PID-OBF and LQR-OBF controllers to setpoint tracking and vibration suppression at the end point of the manipulator. The simulation results are presented in this section. In both cases, the controllers are simulated to manipulator varying payload conditions of 0, 30, 50, and 70g respectively. This is done to test the robustness of both controllers to such variations.

a. Simulation results of the flexible manipulator with LQR-OBF controller

Simulation result of the flexible manipulator to LQR-OBF controller are shown in Figs. 7, 8 and Table 2. The values of the state feedback vector is *K*= [0.873, 63.517, 0.2389, 0.1649]. From the two figures, it can be seen that the LQR controller response remains virtually unchanged for the different payloads considered. From the first figure, it can also be seen that the controller produced no overshoot in all cases while the settling time remained around 9.2seconds as indicated in the table. From the second figure, it can be observed that the deflection also experienced no significant change with the change in payload values as it ranges between $1.4109\text{x}10^{-4}$ - $1.4847\text{x}10^{-4}$ m also as indicated in the table. This shows that the performance of the LQR controller is not much affected by the variation in the payload.

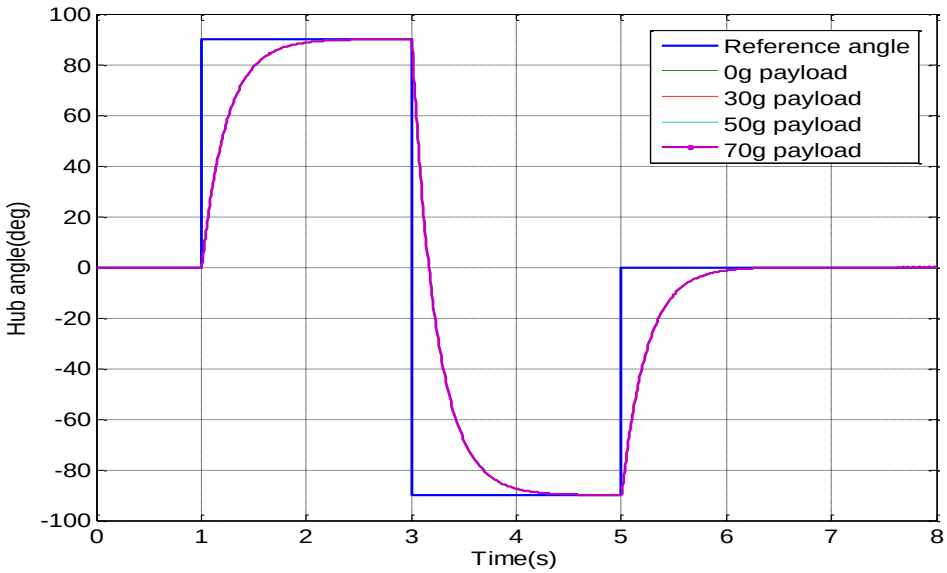

Figure 7. Hub angle response of Flexible manipulator to LQR-OBF controller

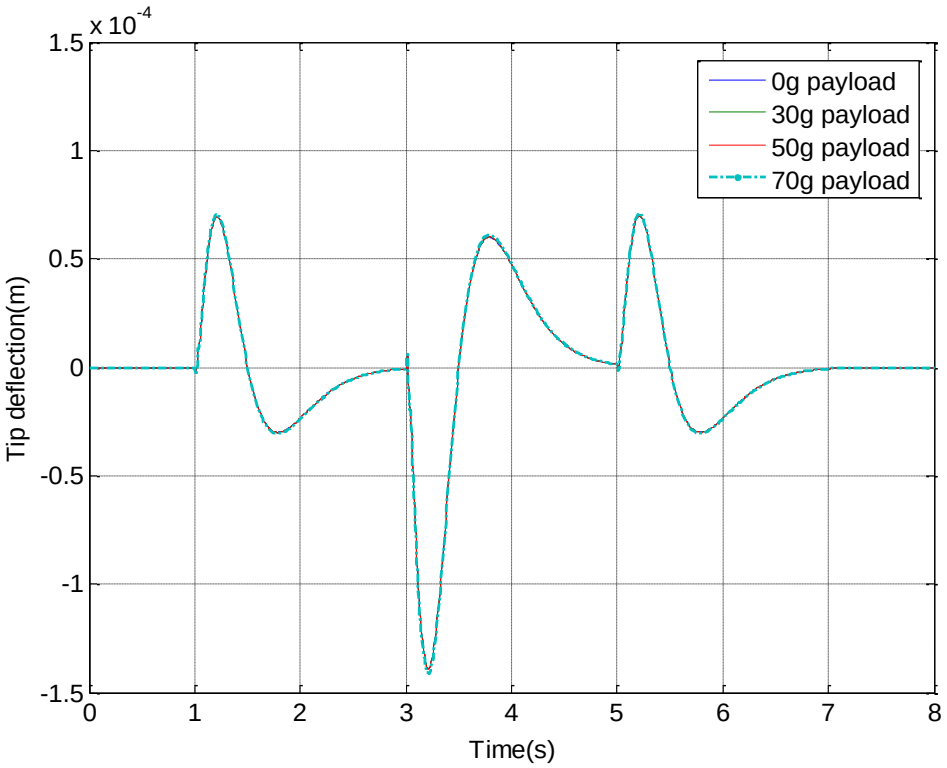

Figure 8. Tip deflection response of the Flexible manipulator to LQR – OBF controller

Table 2: Performance of the LQR – OBF controller to different payloads

Payload (g)	Hub angle Max. Overshoot (%)	Settling Time(s)	Max. Tip deflection(m)
0	0	0.9194	1.4109×10^{-4}
30	0	0.9195	1.4143×10^{-4}
50	0	0.9198	1.4216×10^{-4}
70	0	0.9219	1.4847×10^{-4}

b. Simulation results of the flexible manipulator with PID-OBF controller

Likewise simulation result of the flexible manipulator to PID-OBF controller are shown in Figs. 9, 10 and Table 3. The values of the PID gain used are $K_p=0.22$, $K_i=0.4$ and $K_d=0.9$. From the two figures, it can be seen that the PID controller sensitive to change in the payload values. That is to say, as the payload is increased, the oscillation and overshoot increases. This leads to the values of overshoots shown in Table 2. From the first figure, it can also be seen that the controller produced overshoot in all cases in the range of 6-13.7%. The settling time of the controller is also

affected by the payload as shown in the table. From the second figure, it can be observed that the deflection also experienced significant change with the change in payload values as it ranges between $6.76x10^{-4}$ - $7.855x10^{-4}$ m also as indicated in the table. This shows that the performance of the PID controller is affected by the variation in the payload.

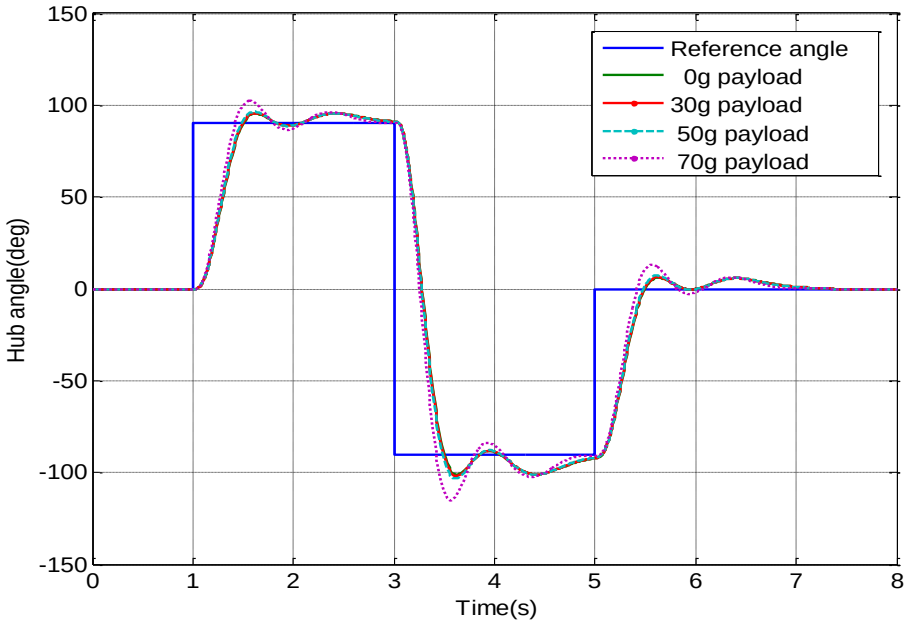

Figure 9. Hub angle using PID – OBF

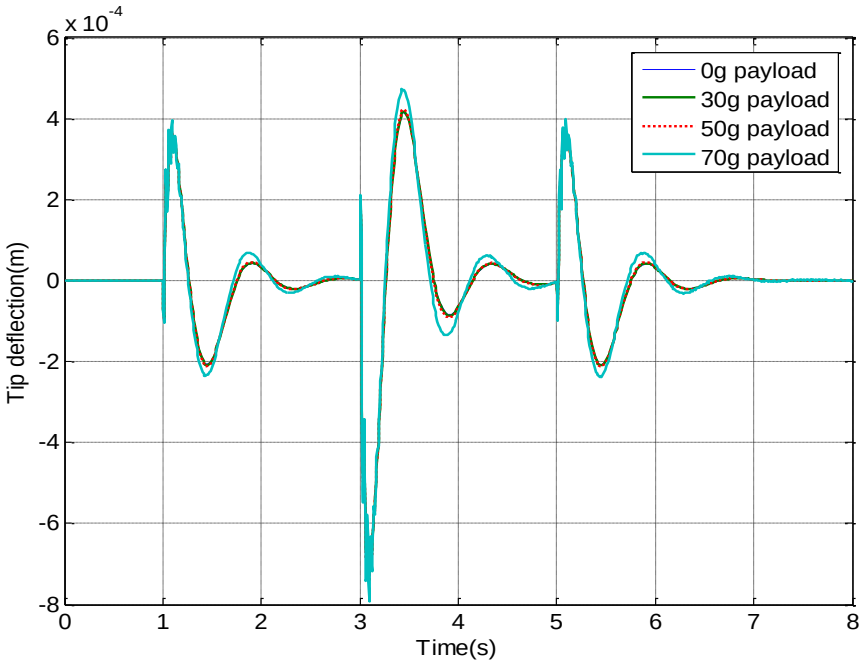

Figure 10. Tip deflection using PID – OBF and PID – OBF

Table 3: Performance of the PID – OBF controller to different payloads

Payload (g)	Hub angle Max. Overshoot (%)	Settling Time(s)	Max. Tip deflection(m)
0	6.0012	1.6993	6.7617×10^{-4}
30	6.3586	1.8378	7.0965×10^{-4}
50	7.1568	1.8577	7.2892×10^{-4}
70	13.7204	1.8681	7.8554×10^{-4}

c. Performance comparison of the LQR-OBF and PID-OBF controllers

To compare the performance of the LQR-OBF and PID-OBF controllers, the flexible manipulator is simulated for the case of 0g payload and results compared in Figs 11 and 12. From these figures, it can be seen that the LQR-OBF controller outperformed the PID-OBF controller in both vibration reduction and setpoint tracking. This further corroborates the results presented in the previous sections.

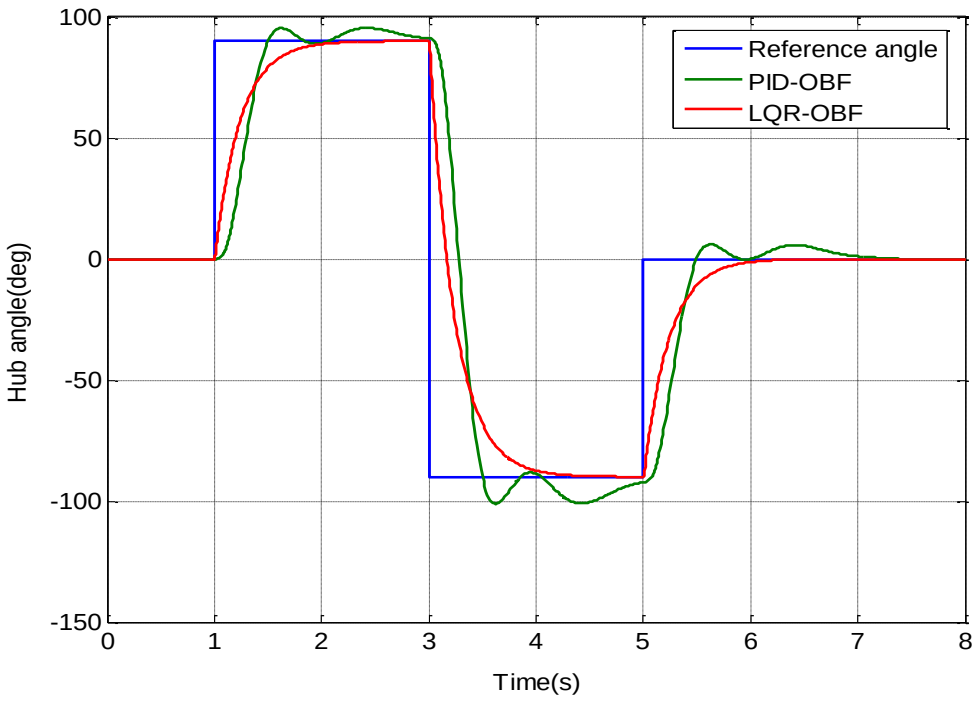

Figure 11. Hub angle using comparison of LQR-OBF

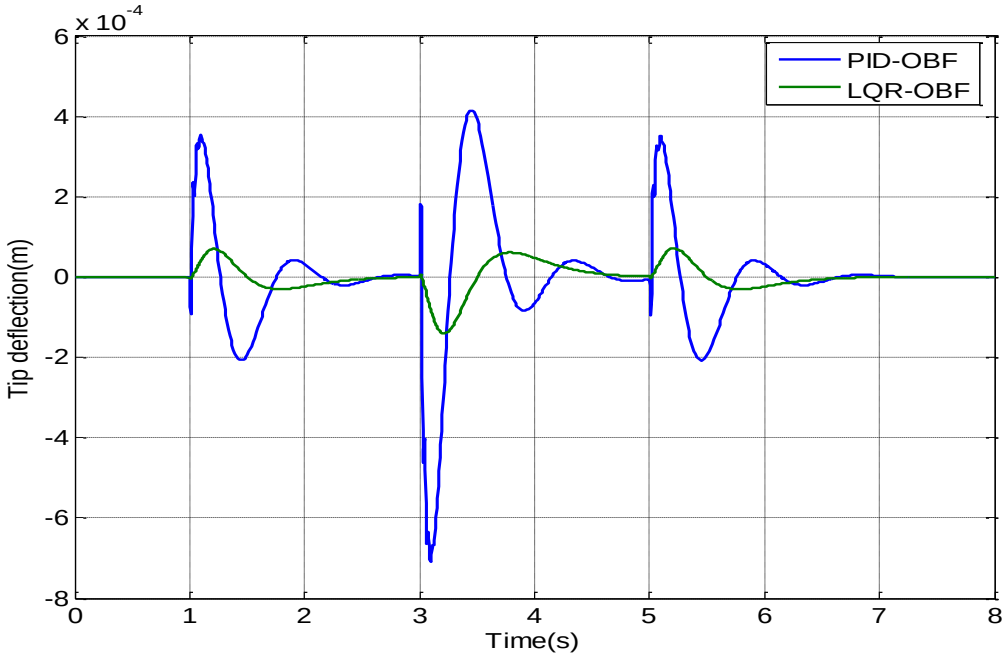

Figure 12. Tip deflection comparison of LQR-OBF and PID-OBF

VI. CONCLUSIONS

This paper has presented the position and residual vibration control of single link flexible manipulator using LQR-OBF and PID-OBF controllers. The performance of the two controllers is compared for robustness against changing payload. Simulation results showed that the LQR-OBF controller performed better than the PID-OBF controller in terms of setpoint tracking and end point vibration suppression as well as robustness to payload variation.

REFERENCES

[1] C. T. Kiang, A. Spowage, and C. K. Yoong, "Review of control and sensor system of flexible manipulator," Journal of Intelligent & Robotic Systems, vol. 77, pp. 187-213, 2015.

[2] Q. Zhang, J. K. Mills, W. L. Cleghorn, J. Jin, and Z. Sun, "Dynamic model and input shaping control of a flexible link parallel manipulator considering the exact boundary conditions," Robotica, vol. 33, pp. 1201-1230, 2015.

[3] Z. Mohamed, A. Chee, A. M. Hashim, M. O. Tokhi, S. H. Amin, and R. Mamat, "Techniques for vibration control of a flexible robot manipulator," Robotica, vol. 24, pp. 499-511, 2006.

[4] M. Ahmad, A. Nasir, N. Pakheri, N. M. Ghani, M. Zawawi, and N. Noordin, "Microcontroller-Based Input Shaping for Vibration Control of Flexible Manipulator System," Australian Journal of Basic and Applied Sciences, vol. 5, pp. 597-610, 2011.

[5] Z. Mohamed and M. O. Tokhi, "Command shaping techniques for vibration control of a flexible robot manipulator," Mechatronics, vol. 14, pp. 69-90, 2004.

[6] Y. Qiang, F. Jing, Z. Hou, and P. Jia, "Residual vibration suppression using off-line learning input shaping method for a flexible joint robot," in Intelligent Control and Automation (WCICA), 2012 10th World Congress on, 2012, pp. 3858-3863.

[7] T. Singh and W. Singhose, "Input shaping/time delay control of maneuvering flexible structures," in American Control Conference, 2002. Proceedings of the 2002, 2002, pp. 1717-1731.

[8] M. Romano, B. N. Agrawal, and F. Bernelli-Zazzera, "Experiments on command shaping control of a manipulator with flexible links," Journal of Guidance, Control, and Dynamics, vol. 25, pp. 232-239, 2002.

[9] Z. Mohamed and M. Tokhi, "Vibration control of a single-link flexible manipulator using command shaping techniques," Proceedings of the Institution of Mechanical Engineers, Part I: Journal of Systems and Control Engineering, vol. 216, pp. 191-210, 2002.

[10] W. Singhose, "Command shaping for flexible systems: A review of the first 50 years," International Journal of Precision Engineering and Manufacturing, vol. 10, pp. 153-168, 2009.

[11] A. Kharola, "A PID Based Anfis & Fuzzy Control of Inverted Pendulum on Inclined Plane (IPIP)," International Journal on Smart Sensing And Intelligent Systems, vol. 9, pp. 616-636, 2016.

[12] S. Mallikarjunaiah and S. N. Reddy, "Design of pid controller for flexible link manipulator," International Journal of Engineering Research and Applications, vol. 3, pp. 1207-1212, 2013.

[13] M. Ahmad, Z. Mohamed, and Z. Ismail, "Hybrid input shaping and PID control of a flexible robot manipulator," Journal of the Institution of Engineers, vol. 72, pp. 56-62, 2009.

[14] Z. Qiu and Z. Zhao, "Pneumatic drive active vibration control for flexible manipulator using an adaptive interactive PD controller," in Robotics and Biomimetics (ROBIO), 2012 IEEE International Conference on, 2012, pp. 1956-1961.

[15] M. A. Ahmad, M. Z. M. Tumari, and A. N. K. Nasir, "Composite fuzzy logic control approach to a flexible joint manipulator," International Journal of Advanced Robotic Systems, vol. 10, p. 58, 2013.

[16] Z. Zhiyong, H. Lvwen, X. Yang, and Z. Xiaoting, "Research on LQR Zone Control Algorithm For Picking Robot Arm," International Journal on Smart Sensing & Intelligent Systems, vol. 7, 2014.

[17] T. Azuma, "Design and experimental verification of state predictive LQG controllers for networked control systems," International Journal on Smart Sensing and Intelligent Systems, vol. 7, pp. 1201-1220, 2014.

[18] M. A. Ahmad and Z. Mohamed, "Techniques of vibration and end-point trajectory control of flexible manipulator," in Mechatronics and its Applications, 2009. ISMA'09. 6th International Symposium on, 2009, pp. 1-6.

[19] M. A. Ahmad and Z. Mohamed, "Modelling and simulation of vibration and input tracking control of a single-link flexible manipulator," Pertanika J. Sci. Technol, vol. 18, pp. 61-76, 2010.

[20] S. Deif, M. Tawfik, and H. A. Kamal, "Vibration and Position Control of a Flexible Manipulator using a PD-tuned Controller with Modified Genetic Algorithm," ICCTA, 2011.

[21] K.-p. Liu and Y.-c. Li, "Vibration suppression for a class of flexible manipulator control with input shaping technique," in Machine Learning and Cybernetics, 2006 International Conference on, 2006, pp. 835-839.

[22] V. Feliu, J. Somolinos, C. Cerrada, and J. A. Cerrada, "A new control scheme of single-link flexible manipulators robust to payload changes," Journal of Intelligent and Robotic Systems, vol. 20, pp. 349-373, 1997.

[23] S. Mahto, "Shape optimization of revolute-jointed single link flexible manipulator for vibration suppression," Mechanism and Machine Theory, vol. 75, pp. 150-160, 2014.

[24] M. O. Tokhi and A. K. Azad, "Modelling of a single-link flexible manipulator system: theoretical and practical investigations," Robotica, vol. 14, pp. 91-102, 1996.

[25] B. A. M. Zain, M. O. Tokhi, and S. M. Salleh, "Dynamic modelling of a single-link flexible manipulator using parametric techniques with genetic algorithms," in Computer Modeling and Simulation, 2009. EMS'09. Third UKSim European Symposium on, 2009, pp. 373-378.

[26] Z. Zhu, K. Liu, Y. He, and J. Han, "An input shaping method based on system output," Sensors & Transducers, vol. 172, p. 254, 2014.

[27] J. Han, Z. Zhu, Y. He, and J. Qi, "A novel input shaping method based on system output," Journal of Sound and Vibration, vol. 335, pp. 338-349, 2015.

[28] N. Singh and S. K. Yadav, "Comparison of LQR and PD controller for stabilizing Double Inverted Pendulum System," International Journal of Engineering, vol. 1, pp. 69-74, 2012.